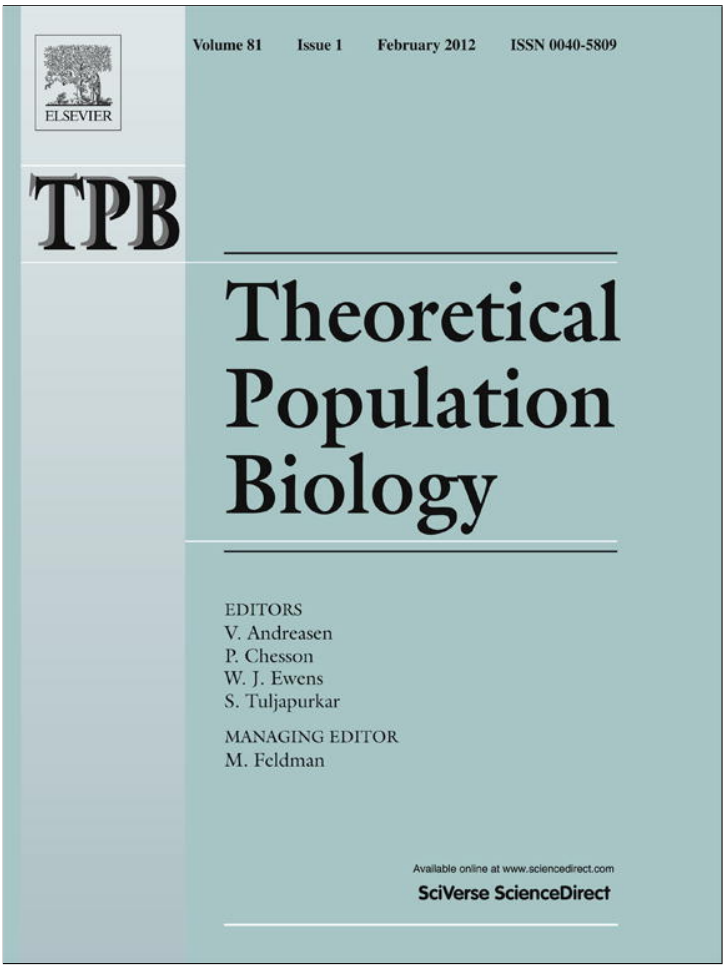

Theoretical Population Biology 81 (2012) 9–19

Contents lists available at SciVerse ScienceDirect

Theoretical Population Biology

journal homepage: www.elsevier.com/locate/tpb

Top-down control in a patchy environment: Revisiting the stabilizing role of food-dependent predator dispersal

Andrew Morozov [a,b,*], Moitri Sen [c], Malay Banerjee [c]

[a] Department of Mathematics, University of Leicester, UK
[b] Shirshov Institute of Oceanology, Moscow, Russia
[c] Indian Institute of Technology, Kanpur, India

ARTICLE INFO

Article history:
Received 12 March 2011
Available online 4 November 2011

Keywords:
Food-dependent migration
Aggregation
Top-down control
Eutrophic ecosystems
Spatial predator–prey model

ABSTRACT

In this paper, we revisit the stabilizing role that predator dispersal and aggregation have in the top-down regulation of predator–prey systems in a heterogeneous environment. We consider an environment consisting of sites interconnected by dispersal, and propose a novel mechanism of stabilization for the case with a non-sigmoid functional response of predators. We assume that the carrying capacity of the prey is infinitely large in each site, and show that successful top-down regulation of this otherwise globally unstable system is made possible through an interplay between the unevenness of prey fitness across the sites and the rapid food-dependent migration of predators. We argue that this mechanism of stabilization is different from those previously reported in the literature: in particular, it requires a high degree of synchronicity in local oscillations of species densities across the sites. Prey outbreaks take place synchronously, but the unevenness of prey growth rates across the sites results in a pronounced difference in the species densities, and so the predator quickly disperses to the sites with the highest prey abundances. For this reason, the consumption of prey mostly takes place in the sites with high densities of prey, which assures an efficient suppression of outbreaks. Furthermore, when the total size of prey population is low, the distribution of both species among the sites becomes more even, and this prevents overconsumption of the prey by the predator. Finally, we put forward the hypothesis that this mechanism, when considered in a tri-trophic plankton community in the water column, can explain the stability of the nutrient-rich low-chlorophyll open ocean regions.

1. Introduction

In this paper, we revisit the role of predator or parasitoid aggregation and dispersal in stabilizing predator–prey and parasitoid–host interactions. We consider an environment consisting of a number of interconnected sites with an exponential growth rate of prey in each site, and local predation described by a non-sigmoid functional response with saturation (Holling types I, II), which is a quite common situation observed in nature both for predator–prey and host–parasitoid interactions (Holling, 1959; Hassell, 1978; Abrams, 1990; Scheffer and De Boer, 1995; Jeschke et al., 2002). Classical works predict that the local dynamics in this case should be intrinsically unstable (e.g., Oaten and Murdoch (1975)), and thus long-term local persistence of species is impossible in the absence of dispersal between sites.

Overall, the central idea that the interplay of spatial subdivision, species dispersal and predator or parasitoid aggregation can assure persistence and stability of such globally unstable systems has a long history starting from the seminal papers of Hassell and May (1973, 1974). Since then a large number of publications have appeared considering different mechanisms of stabilization and persistence in such systems (Chesson and Murdoch, 1986; Godfray and Pacala, 1992; Ives, 1992; Murdoch et al., 1992; Rohani et al., 1994; Briggs and Hoopes, 2004; Weisser et al., 1997; Nachman, 2006; Abta and Shnerb, 2007). Along with other scenarios of stabilization, it was hypothesized that asynchrony in the oscillations of species densities on sites would play a pivotal role in promoting successful top-down control (Ives, 1992; Murdoch et al., 1992; Briggs and Hoopes, 2004). In such systems, the dispersal of species from more populous sites to less populous ones can dampen local oscillations and result in stabilization. A permanent existence of dynamical sinks characterized by low species densities is guaranteed by asynchrony of local oscillations on the sites (Ives, 1992).

In this paper, we will consider predator–prey or parasitoid–host ecosystems in a patchy environment, and present a mechanism

* Corresponding author at: Department of Mathematics, University of Leicester, UK.
E-mail addresses: am379@leicester.ac.uk, am379@le.ac.uk (A. Morozov).

0040-5809/$ – see front matter © 2011 Elsevier Inc. All rights reserved.
doi:10.1016/j.tpb.2011.10.003

of stabilization, which has not been explicitly reported in the literature so far. An interesting particularity of our proposed mechanism is that the stabilization requires a high degree of *synchrony* in the oscillations of species densities in sites. We will show that a successful top-down regulation of this kind becomes possible due to a combination of the unevenness of species fitness across the sites (e.g., different growth rates of prey) and rapid food-dependent migration of predators between the sites. In this paper, we provide both a conceptual explanation and the analytical proof of stabilization and persistence in the ecosystem with the necessary conditions being: the recourse distribution for prey or pest across sites must be uneven; the distribution of predators in the sites should be quickly adjusted to the distribution of food and, finally, the saturation in the local functional response of predator needs to be low.

Interestingly, stabilization according to the reported mechanism is not only limited to two-component predator–prey systems, it can also take place in a case of tri-trophic food webs including a prey, an intermediate predator and a top predator. We show that fast migration of the top predator can stabilize otherwise unstable oscillations of the prey and its intermediate predator in each site. Regulation in such tri-trophic food web has several important ecological applications: for instance, understanding the dynamics of phytoplankton–microzooplankton–mesozooplankton in the water column (Irigoien et al., 2005). We suggest that the low phytoplankton density observed in the so-called nutrient-rich low-chlorophyll open ocean regions (Chavez et al., 1990; Armstrong, 1994; Boyd, 2002) can be explained based on our proposed mechanism of regulation.

The paper is organized as follows. In Section 2 we present the general model by explicitly describing local predator–prey interactions in a patchy environment and migration between the patches. Based on the assumption that migration of predators is a fast process, we simplify the initial full model by reducing the number of equations. In Section 3, we analyze this reduced model, and show that the predator–prey system with an unlimited carrying capacity can be stabilized via top-down control. In Section 4, we generalize the previous results on stability by considering a tri-trophic food web model. Finally, in Section 5, we discuss the previously demonstrated mechanisms of stabilization, along with ecological applications of the results including the stabilization of plankton communities with eutrophication.

2. The general modeling framework

We consider trophic interactions in a patchy environment consisting of n sites. All sites are connected via continuous migration of species. In the simplest case, the food-web consists of only two trophic levels. In site i, the variation of the biomass of prey P_i and its predator Z_i is described by the following system of ODEs

$$\frac{dP_i}{dt} = \varepsilon(r_i P_i - f(P_i)Z_i), \quad i = 1, n, \tag{1}$$

$$\frac{dZ_i}{dt} = \sum_j \tilde{m}_{ij} Z_j + \varepsilon(kf(P_i)Z_i - m_i Z_i), \quad i = 1, n, \tag{2}$$

where the terms $\tilde{m}_{ij}$ stand for *per capita* migration rates of predator from site j to site i, respectively. Here we neglect the migration of prey individuals by assuming them to be sessile; however, in the Discussion section we shall briefly address the potential influence of migration of prey on the system stability. We suggest that $\tilde{m}_{ij}$ are not constant, but instead depend on the amount of food in the site. The functions $r_i(P_i)$ are *per capita* prey growth rates; $f(P)$ is the functional response of predator; k is the efficiency coefficient describing the transformation of the consumed prey into the biomass of predators; m_i is the *per capita* mortality rate of the predator, which is considered to be constant and the same for all sites, $m_i = m$. All functions in the right-hand side parts of (1)–(2) are assumed to be continuously differentiable. The dimensionless coefficient $\varepsilon \ll 1$ is introduced to take into account a slower scale of population dynamics compared to the fast migration processes.

In this paper, we assume that the prey growth in the absence of a predator is unlimited ($r_i = \text{const}$, which means that the carrying capacity of prey is infinite) and that the functional response of the predator is of Holling type II. To parameterize Holling type II response, we use the classical Monod function (Holling, 1959)

$$f(P) = \alpha \frac{P}{1 + \beta P}, \tag{3}$$

where α, β are positive parameters with an obvious meaning.

We shall consider that the migration rates of the predator $\tilde{m}_{ij}$ are prey-dependent. We should say that there exists a variety of parameterizations of $\tilde{m}_{ij}$ in the literature (e.g., Ives, 1992; Murdoch et al., 1992; Bernstein et al., 1999; El Abdllaoui et al., 2007). Here we assume that the rates at which predators leave a given site are decreasing functions of prey biomass since the predator is more willing to stay in a site with a high amount of food compare to a poor food site. Also, we assume that the immigration rates of predators do not depend on amounts of prey in other sites. In other words, we suggest that predators do not possess the information on the food abundance in other sites. The simplest possible parameterization of this scenario gives

$$\tilde{m}_{ij} = \mu \frac{1}{\nu P_j + 1}, \qquad \tilde{m}_{ii} = -(n-1)\,\mu \frac{1}{\nu P_i + 1}, \quad i = 1, n \tag{4}$$

where υ and μ are certain positive constants. The multiplier $(n-1)$ in front of the terms $\tilde{m}_{ii}$ describes the fact that the flux of animals leaving site i are evenly re-distributed among the other sites $i \neq j$.

We shall consider that the migration is a fast processes compared to the characteristic time scale of the population dynamics. This signifies that $\varepsilon \ll 1$. Such a situation is commonly observed in nature (Godin and Keenleyside, 1984; Jakobsen and Johnsen, 1987; Cuddington and McCauley, 1994; Larsson, 1997; Pulido and Díaz, 1997; Lampert, 2005; Morozov and Arashkevich, 2008). Assuming migration to be a fast process we can reduce the number of variables (Auger et al., 2000). We first set $\varepsilon = 0$. In this case, the total biomass of predators as well as the biomasses of prey in each site remain constant. Due to a rapid migration, the distribution of the predators among the sites quickly attains its equilibrium $\{\tilde{Z}_i\}$ which can be determined by equating migration terms in (2) to zero

$$\sum_{i \neq j} \mu \frac{1}{\nu \tilde{P}_j + 1} \tilde{Z}_j - n\mu \frac{1}{\nu \tilde{P}_i + 1} \tilde{Z}_i = 0, \quad i = 1, n. \tag{5}$$

We use the symbol "~" for the prey biomass in the sites as well to unify the notation. It is easy to compute the explicit expressions for the re-distribution of predators $\tilde{Z}_i$

$$\tilde{Z}_i = \frac{1 + \nu \tilde{P}_i}{\nu \sum_i \tilde{P}_i + n} Z, \quad i = 1, n, \tag{6}$$

where $Z = Z_1 + Z_2 + \cdots + Z_n$ is the total biomass of predators in the ecosystem.

On a slow time scale $\tau = t\varepsilon$ (the demographic time scale) the full model (5)–(6) can be re-written in the following reduced form

$$\frac{d\tilde{P}_i}{d\tau} = r_i \tilde{P}_i - f\left(\tilde{P}_i\right) \tilde{Z}_i + O(\varepsilon), \quad i = 1, n \tag{7}$$

$$\frac{dZ}{d\tau} = k \sum_i f\left(\tilde{P}_i\right) \tilde{Z}_i - Zm + O(\varepsilon), \tag{8}$$

where $\tilde{Z}_i$ is defined by (6). One can see that the model now contains $n+1$ equations instead of $2n$ as in the initial model. We shall further omit the symbol "~" for convenience when analyzing the simplified model. Further on, to be able to obtain some analytical results and keep the equations tractable, we shall consider that $\nu P_j \gg 1$, i.e., we neglect the term describing food-independent migration of predators. Thus, the instantaneous spatial distribution of predators will be given by

$$\tilde{Z}_i = \frac{P_i}{\sum_i P_i} Z. \tag{9}$$

As the result, the instantaneous distribution of predators follows the relative distribution of resources. Note that such distribution can model a number of field observations relatively well (Milinski, 1979; Godin and Keenleyside, 1984; Jakobsen and Johnsen, 1987; Cuddington and McCauley, 1994; Larsson, 1997; Lampert, 2005; Morozov et al., 2011).

3. Trophic regulation by a fast-moving predator

Substituting the instantaneous distribution of predators (9) into model (7)–(8) gives

$$\frac{dP_i}{d\tau} = r_i P_i - f(P_i)\frac{P_i}{\sum_i P_i} Z, \quad i = 1, n \tag{10}$$

$$\frac{dZ}{d\tau} = \left(k \sum_i f(P_i)\frac{P_i}{\sum_i P_i} - m \right) Z. \tag{11}$$

Model (10)–(11) has a trivial stationary state where the biomass of all species is equal to zero, but it is easy to prove that this stationary state is always unstable. The same holds true for all stationary states for which the biomass of prey in some sites is zero (semi-trivial states). This follows from the exponential growth of prey which always takes place for small P_i. It can be proved (see Appendix A) that system (10)–(11) has a unique interior stationary state with all species biomass being above zero. The stationary total biomass of predator Z^* is computed in Appendix A. The stationary biomass of prey in each site can be computed only numerically. Our bifurcation analysis of (10)–(11) shows the existence of a variety of dynamical regimes, the number of possible patterns increasing with the number of sites n. In this paper, however, we shall consider in detail the cases when $n = 2, 3$.

Fig. 1A shows a bifurcation diagram in the $r_1/r_2 - \beta$ plane for the two-site model. The ratio r_1/r_2 represents the degree of heterogeneity of the environment. The corresponding dynamical regimes are represented schematically as two-dimensional pseudo-phase portraits. The diagram is constructed with the help of the software MATCONT (Dhooge et al., 2003). There are two dynamical regimes (parametric domains 1 and 2), where the model has attractors (a stable stationary state or a stable limit cycle, respectively). In domain 3, model trajectories always go to infinity regardless of the initial conditions. The solid line is a Hopf bifurcation curve; the internal stationary state changes its stability when crossing this curve. The dotted curve is a cycle bifurcation curve: on this curve a collision between an unstable and a stable cycle takes place. The point O_1 is a co-dimension two generalized Hopf bifurcation point (Bautin point) where the first Lyapunov coefficient vanishes (Kuznetsov, 1995). Computation of the second Lyapunov coefficient shows that $l_2 < 0$ which signifies the appearance of two enclosed limit cycles, the inner one being stable.

The bifurcation diagram in Fig. 1A shows that a predator–prey system with an unlimited carrying capacity for prey becomes regulated (the system trajectories become bounded, see domains 1 and 2). We have proven analytically (see Appendix B) the stability of the interior stationary state for the case where functional response is linear (i.e., $\beta = 0$). The stability of the interior equilibrium for $\beta = 0$ signifies that such stability will remain for a small-magnitude perturbation of the system by adding saturation $0 < \beta \ll 1$ since the system is structurally stable. A pronounced saturation in functional response (large β), however, would result in a system destabilization; trophic regulation becomes impossible resulting in unbounded trajectories (domain 3). Another crucial condition for a top-down control is unevenness of properties of sites resulting in unequal prey growth rates: for the equal growth rates of prey the equilibrium is always unstable (see Appendix C). Finally, we should say that for any $\beta > 0$ there exist some unbounded trajectories; thus the success of the trophic regulation depends on the initial conditions. The basin of attraction for the interior equilibrium is large for $\beta \ll 1$ (the system is globally stable for $\beta = 0$) and it shrinks with an increase in β.

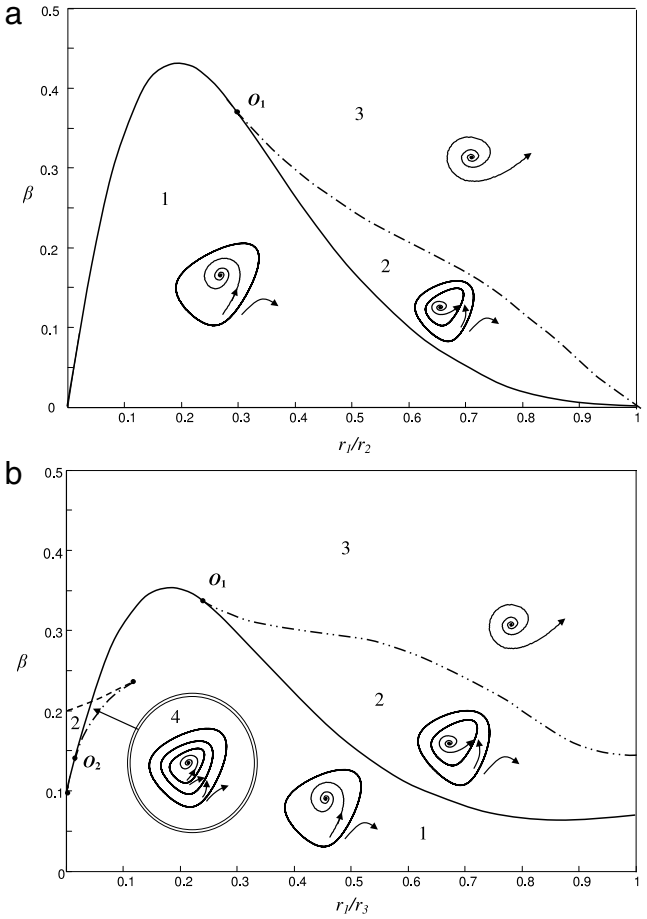

Fig. 1. Two parametric bifurcation diagrams for model (10)–(11). Dynamical regimes are shown schematically by pseudo-phase portraits (for details see the text). The system can be regulated in domains 1, 2 and 4. The solid curve is the Hopf bifurcation curve. The dot-dashed curves represent limit cycle bifurcation curves. The points O_1 and O_2 are co-dimension two general Hopf bifurcation (Bautin) points. (A) Bifurcation diagram is constructed for $n = 2$ (two-site model); (B) bifurcation diagram is constructed for $n = 3$ (three-site model), $r_2 = 0.6$. The other parameters are $\alpha = 2, k = 0.25, m = 0.1, r_1 = 1$.

An increase in the number of sites in the habitat results in an increase of the system complexity. This can be already seen from the bifurcation diagram (Fig. 1B) constructed for $n = 3$. In particular, another regime – implying coexistence of three enclosed limit cycles – appears (domain 4). The main result that a successful grazing control in the system with unlimited carrying capacity is possible remains. Moreover, one can see that the general structure of the diagram is similar to the one shown in Fig. 1A. In

particular, the interior equilibrium is stable in case the saturation of predation is not pronounced and the interior stationary state is always unstable for the even prey fitness in the sites $r_1 = r_2 = r_3$. We have proven analytically the two mentioned statements based on the Routh–Hurwitz stability criterion (not shown). Note that unlike in a two-site habitat, the stability of the system in a three-site habitat can be observed in case $r_1 = r_3$ ($r_1 > r_2$) since the system eventually evolves to a two-site model, which allows stability of the interior stationary state.

A further increase of the number of sites does not affect the main findings obtained for $n = 2, 3$: regulation of the system requires an uneven growth rate across the sites and saturation in the functional response β should be small. Overall, the number of different patterns of dynamics, as multiple cycles, increases with n, however, parametric domains corresponding to these new patterns are small compared to those of regimes 1, 2, 3 in Fig. 1. In the limiting case $n \to \infty$, it becomes more convenient to consider the system as continuous and spatial subdivision in terms of a certain parameter θ. For instance, this can be the spatial location sites. In this paper, we do not analyze this case since the outcome would largely depend on a concrete functional dependence of prey fitness on the parameter θ and should be done elsewhere (cf. Morozov (2010)). For the same reason, it is hardly possible to draw conclusions on the influence of n on the degree of stability in the system (cf. Ives, 1992).

4. Trophic regulation by a fast-moving top predator

In the previous section, we analyzed conditions for stabilization in a two-level food-web. Such a simple system, however, is often a simplification of reality since the prey population is, in turn, a predator or consumer with respect the lower trophic level. In this case, we have a food chain consisting of a top predator Z, an intermediate predator $P$and a prey N. The dynamics of such a tri-trophic linear food web are described by

$$\frac{dN_i}{d\tau} = r_i N_i - f_N(N_i) P_i, \tag{12}$$

$$\frac{dP_i}{d\tau} = k_N f_N(N_i) P_i - Z_i f(P_i), \tag{13}$$

$$\frac{dZ}{d\tau} = k \sum_i f(P_i) Z_i - mZ, \tag{14}$$

where N_i is the biomass of species of the lowest trophic level in site i. We consider that the natural mortality of P_i is much smaller than the mortality caused by the top predator; $f_N(N)$ and k_N are the functional response and the efficiency coefficient, respectively, of the intermediate predator P_i. As previously, we assume that rapid migration of Z_i results in the distribution of $\{Z_i\}$ following the distribution of food and we neglect migration of the intermediate predator. Note that the scenario described by (12)–(14) is by no means exotic in nature. An important study case includes tri-trophic regulation in eutrophic planktonic marine food-webs (see Discussion).

Analysis of the full tri-trophic food web model (12)–(14) is a rather complicated matter and should be done elsewhere in all detail for an arbitrary n. In this paper, we shall consider an important particular case where the top predator grows on a slow time scale (compared to the characteristic growth rate of the lower trophic levels) and we can assume its biomass to be constant. In this case, the previous model can be re-written as

$$\frac{dN_i}{dt} = r_i N_i - \frac{a_N N_i}{1 + b_N N_i} P_i, \quad i = 1, n \tag{15}$$

$$\frac{dP_i}{dt} = k_N \frac{a_N N_i}{1 + b_N N_i} P_i - M \frac{P_i^2}{1 + \beta P_i} \frac{1}{\sum_i P_i}, \quad i = 1, n \tag{16}$$

where the product $M = \alpha Z$ becomes a system parameter; a_N, b_N are the parameters describing the functional response of the intermediate predator.

Further on, we shall focus mostly on the case $n = 2$, the resultant model (15)–(16) being a four-dimensional system. The system has the trivial equilibrium (0, 0, 0, 0) which is always unstable. The same concerns the semi-trivial equilibria, where the biomass of one species (or more species) is zero. One can easily prove that the system may have no more than one interior stationary state with positive biomasses of all species. We shall be further interested in attaining stability of the interior stationary state which would signify a successful top-down control of the system.

Fig. 2 provides an insight into the structure of the parametric space of model (15)–(16). Fig. 2A shows the bifurcation diagram in the $r_1/r_2 - \beta$ plane. The corresponding dynamical regimes are shown schematically and have the same meaning as in Fig. 1. One can see that the stabilization of the system by the fast-moving top predator becomes possible only in the case of uneven fitness on the sites. The functional response of the top predator should not be largely saturated (small β are required). Unlike regulation in the predator–prey system (10)–(11), even for a linear functional response of the top predator stabilization becomes possible only within a limited range of the extrinsic environmental heterogeneity modeled by r_1/r_2. This can be explained by the fact that there is saturation in the functional response $f_N(P_i)$ for the intermediate predator and this has a destabilizing effect on the system. We found analytically (see Appendix D) that in the case where the functional responses of the top and the intermediate predators are linear ($b_N = 0$; $\beta = 0$), the interior stationary state is always stable, thus this assures stability for a small saturation in functional responses ($b_N \ll 1$; $\beta \ll 1$).

Fig. 2B shows the influence of the total amount of the top predator in the system M, on the possibility of regulation. One can see from the diagram that a large total amount of top predator will result in overgrazing and destabilization. Note that system (15)–(16) can be stabilized even for $M = 0$, i.e., in the absence of top predators. However, it is a mathematical artifact: adding a small natural mortality $m_P > 0$ for the intermediate predator will correct this artifact by assuring the existence of a narrow band of domain 3 coming inside domain 1 and separating the stability domain 1 from the axis $M = 0$. Note also that a pronounced saturation in the functional response of the intermediate predator (large b_N) will result in the situation where persistence of species is impossible: the only domain in the M–r_1/r_2 plane will be domain 3.

Note that considering the dynamics of the full model (12)–(13) enhances the stability of the system. In particular, domain 1increases in size and stable equilibrium of all three species is possible within a larger range of the ratio r_1/r_2 (not shown). We should also say that increasing the number of sites n in the system does not qualitatively alter the main results on stabilization.

5. Discussion and conclusions

We have proposed a novel mechanism of stabilization for predator–prey and parasitoid–host interactions in an environment consisting of interconnected sites. We have shown that the following features are required to assure species persistence in an otherwise globally unstable system. Firstly, the spatial distribution of resources affecting the growth rate of prey should be uneven among the sites. Secondly, the mechanism requires a rapid food-dependent migration of predators, causing the predators' distribution to instantaneously follow the distribution of prey. Finally, the local functional response of the predator in the sites should be close to linear, thus the predator handling time should be sufficiently small.

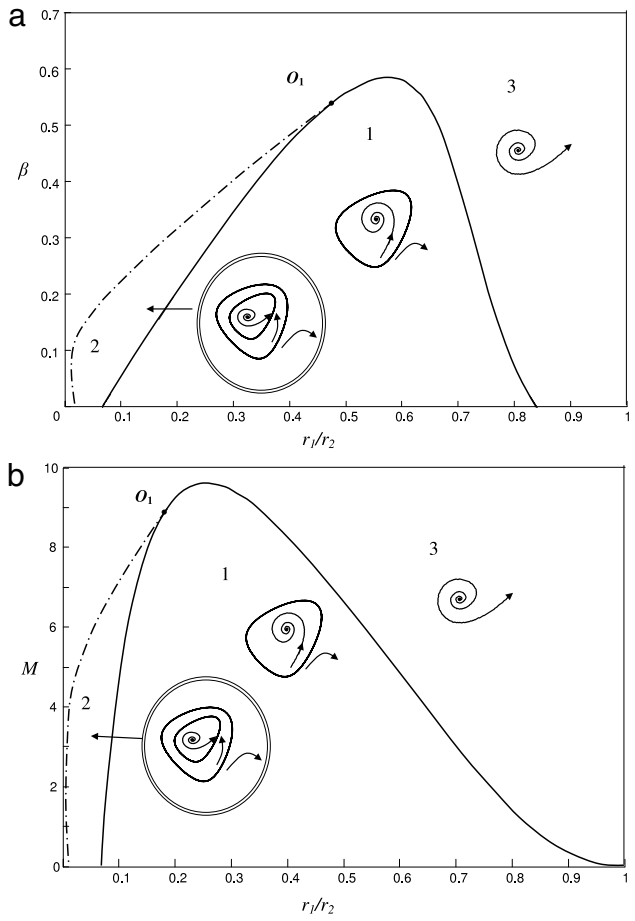

Fig. 2. Two parametric bifurcation diagrams for model (16)–(17), $n = 2$. Dynamical regimes are shown schematically by pseudo-phase portraits. The system can be regulated in domains 1 and 2. The solid curves are Hopf bifurcation curves. The dashed line depicts limit cycle bifurcation curves. (A) $M = 1$; (B) $\beta = 0.1$. Other parameters are $a_N = 2$, $b_N = 0.03$; $k_N = 0.25$, $m = 0.1$, $r_1 = 1$.

5.1. Revealing the mechanisms of stabilization

The stabilizing role of the aggregation of predators or parasitoids in the regulation of predator–prey and parasitoid–host systems has been previously discussed in a large number of publications. The central idea of the stabilizing behavior of parasitoid aggregation comes back to the seminal papers of Hassell and May (1973, 1974) in which the authors analyzed the scenario of regulation where the relative proportions of hosts on the sites were always constant in time, and the distribution of parasitoids followed that of hosts. They suggested that such parasitoid aggregation was responsible for stabilization of host–parasitoid systems, an idea which was developed in a number of further papers (Beddington et al., 1978; May and Hassell, 1981; Hogarth and Diamond, 1984). Later on, however, Chesson and Murdoch (1986) demonstrated that the 'aggregation of parasitoids to host density' was not actually the mechanism of stabilization, since parasitoid aggregation independent of local host density could also result in stabilization. In fact the stabilizing force was seen to be spatial variation in the risk of parasitism faced by the hosts (Chesson and Murdoch, 1986; see also Hassell et al., 1991; Hassell, 2000). Interestingly, the conclusion on the stabilizing role played by the aggregation of parasitoids can largely depend on the actual definition of the term of aggregation, where one should distinguish between statistical-based and behavioral-based definition (Murdoch and Stewart-Oaten, 1989; Godfray and Pacala, 1992). We should also emphasize that the stabilizing or destabilizing effects of parasitoid or predator aggregation is determined by the particular choice of model: for instance, it would strongly depend on whether or not the within generation redistribution of species was included (Rohani et al., 1994).

Along with spatial aggregation of parasitoids or predators, another important factor which can influence stabilization is heterogeneity of the physical environment resulting, in unevenness of species fitness across sites (Ives, 1992; Murdoch et al., 1992); see also Abta and Shnerb, 2007. It was shown that unevenness of sites could promote stabilization of ecosystems, with the major factor assuring the stabilization being the asynchrony in the species oscillations on different sites. The role of asynchrony in this case was to create dynamical sinks and sources which dampen local oscillations with too high or too small population densities. As a result, the dispersal of species from highly populated to sparsely populated sites is intensified at peak of densities of the highly populated sites, since the density in low population sites is near its minimal value (Ives, 1992). The difference of species fitness among the sites is necessary to assure a permanent asynchrony of local oscillations, thus providing dynamical sinks. Finally, in other works (Weisser and Hassell, 1996; Weisser et al., 1997) it was suggested that ecosystem stabilization is possible because the dispersal of organisms is not an instantaneous process but requires a long time so that there should always exist a large pool of dispersers which are currently in transit between sites (and thus are not involved in local interactions), which could result in different scenarios of stabilization.

Interestingly, the mechanism of ecosystems' regulation proposed in our paper is somewhat different from the previously reported ones. In our case the stabilization becomes possible via *synchronous* oscillations of species across the sites. In Fig. 3A we show an example of such damped oscillations of species densities in model (10)–(11) constructed for $n = 2$, $\alpha = 1$, $k = 0.25$, $m = 0.1$, $r_2 = 1$, $r_1 = 0.3$. One can see that the trajectory will eventually approach the stationary stable state. Interestingly, an artificial desynchronization of species oscillations across the sites can result in the loss of stability, as we will discuss in the next section.

It is possible to come up with a simple (but not mathematically strict) explanation of the observed mechanism of stabilization. During an outbreak of prey biomass, the local density of the prey in each site increases simultaneously. However, due to unevenness of the prey fitness across the sites, the prey density will be larger in sites with higher prey growth rates, and lower in those with poor fitness. Since the predator quickly follows the relative proportion of food distribution among the sites, it migrates to sites with highest food abundances and the maximal consumption of prey takes place on those sites. The arrival of this extra amount of consumers on sites with higher abundance of prey allows for dampening of outbreaks. In the case of a low total amount of prey in the system, the densities of the prey as well as those of the predator are distributed more evenly among the sites, thus preventing overconsumption of prey by predators.

Note that the described mechanism of stabilization is similar to the recently reported alteration between the global and local functional responses of predators (Morozov and Arashkevich, 2008; Morozov, 2010): a sigmoid global functional response of a predator population can emerge from non-sigmoid local functional responses. This can be illustrated in the given model via a direct computation of the global functional response of the predator population $F(P)$ which is defined as the total consumption rate per predator biomass

$$F(P) = \frac{\sum\limits_i P_i f(P_i) Z}{Z \sum\limits_i P_i} = \frac{\sum\limits_i P_i f(P_i)}{P}, \quad P = \sum_i P_i. \tag{17}$$

Since oscillations in different sites are synchronized we can approximately describe the dynamics in terms of the average

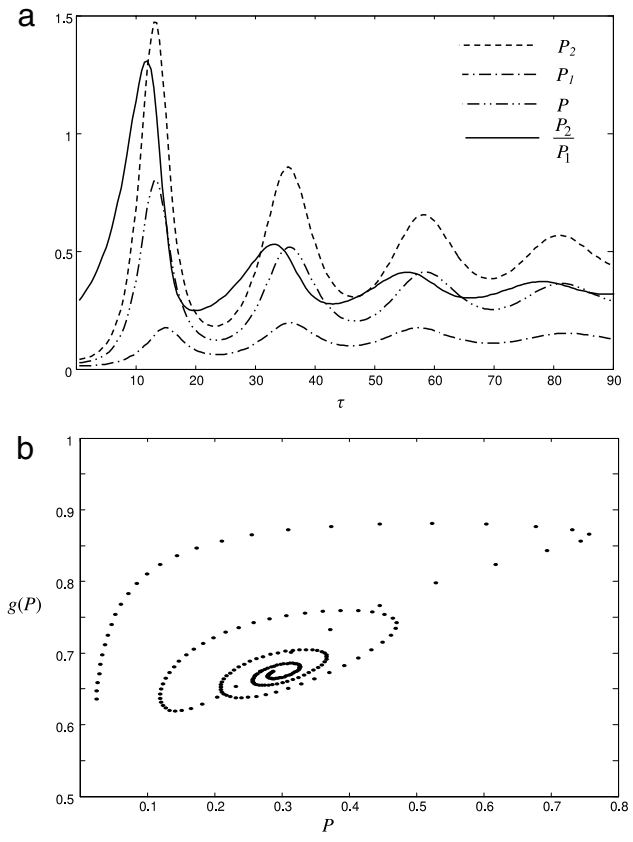

Fig. 3. Explaining stabilization in model (10)–(11), $n = 2$. (A) Temporal oscillations in the species densities P_1, P_2, the average biomass of prey P, and the ratio P_2/P_1 (which is rescaled by multiplying by 0.1 to fit the graph). Other parameters are $\alpha = 1$, $k = 0.25$, $m = 0.1$, $r_2 = 1$, $r_1 = 0.3$. Oscillations of species in the sites are synchronized. The trajectory eventually approaches the stable stationary states r_2r_1(B). The global clearance rate $g(P) = F(P)/P$ for the consumption of prey population by the predator population plotted against the average prey density P. The clearance rate is constructed using model trajectories from (A). Increase of $g(P)$ in a large portion of plot indicates a Holling type III global functional response which enhances the stability of the system (Murdoch and Oaten, 1975).

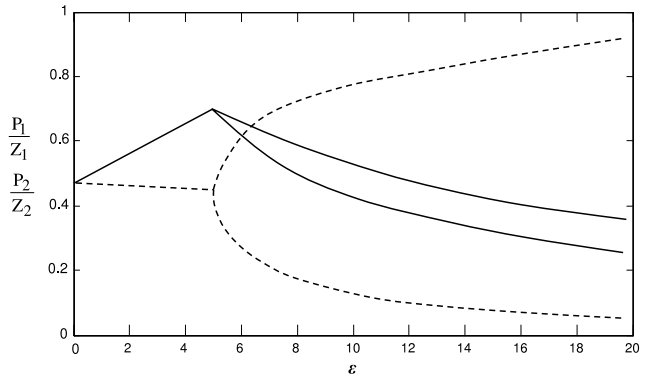

Fig. 4. Dynamics of the full model (1)–(2) with $\varepsilon > 0$, $n = 2$. Testing the hypothesis that the distribution of predators across the sites follows the distribution of prey (see expression (9)) for $\varepsilon > 0$. The actual ratios P_1/Z_1 (dashed line) and P_2/Z_2 (solid line), corresponding to the system attractor, are plotted as function of ε. The model parameters are $\alpha = 1$, $k = 0.25$, $m = 0.1$, $r_1 = 1$, $\beta = 0.15$. The parameters, describing the migration of predators (4) are $\mu = 10$, $\upsilon = 0$. Increasing in ε results in a violation of the distribution of predators (9); however, regulation of the system (bounded trajectories) is still possible.

biomasses P and Z. The stability of the resultant two-component predator–prey P–Z system is determined by the quantity $g(P) = F(P)/P$ called also the clearance rate: in the case that $g(P)$ is an increasing function of P, the predator–prey coexistence equilibrium is stable (Murdoch and Oaten, 1975). Fig. 3B shows the clearance rate plotted using the model trajectories in Fig. 3A. One can see that an increase in P, which corresponds to a synchronous increase in all P_i, will correspond to an increase in $g(P)$. This signifies that the global functional response of the predator population shows an accelerating growth rate as a function of total amount of food, thus assuring the system's stability (Murdoch and Oaten, 1975). Note that due to the fact that the total biomass P does not exhaustively characterize the system, we have several 'branches' of $g(P)$ in the figure in the course of time while we approach the equilibrium. We should emphasize that a rigorous mathematical proof of stabilization can be also performed by implementing stability analysis of the stationary state (see Appendix B).

The synchrony of oscillations of prey densities in different sites plays a crucial role in this system's stabilization, and therefore an important question concerns the mechanism leading to in-phase oscillations. Here we provide only a qualitative explanation of this phenomenon. Oscillations of the prey densities in different sites are synchronized by the quick re-distribution of predators, which follows the relative proportion of food, and as a result of this, an out-of-phase oscillation mode becomes unstable. Let us, for the sake of simplicity, consider a predator–prey model (10)–(11) with $n = 2$. An out-of-phase oscillation in this case signifies that the total rates of change of the prey densities (including predation) have different signs during a large part of the period of oscillations. Consider, for example, the case where the rates of change of prey in sites 1 and 2 are negative and positive, respectively. Regardless of the sign of the predator growth rate, a further decrease in the prey biomass in site 1 and a simultaneous increase of prey biomass in site 2 will result in a release of predation pressure in site 1, and thus in an increase of the per-capita rate of change of P_1. Similarly, an increase in the prey density in site 1 and the simultaneous decrease of prey density in site 2 will result in intensification of predation in site 2 and, thus, in a decrease of the per capita growth rate of prey in site 2. As a result, under the permanent influence of this negative feed-back, the out-of-phase oscillation mode will eventually be damped. On the other hand, synchronous oscillations are characterized variation of the prey rate of change in different sites having a less pronounced impact. The reason for this is that the variation of the predation rates will be smaller when the species densities are oscillating in phase, as the relative amounts of predators are determined by the ratios of prey densities in the sites. Thus, the synchronous oscillation mode in the system will eventually outcompete the asynchronous mode.

The above explanation of the stabilization of the system depends on the fact that re-distribution of predators among the sites is fast. In terms of the general model (1)–(2), this signifies that $\varepsilon \to 0$, but a direct simulation of the full system with $2n$ equations shows, surprisingly, that stability remains up to relatively large values of ε. This can be seen, for example, in Fig. 4 (constructed for (10)–(11), $n = 2$) showing the evolution of the ratios P_1/P_2 and Z_1/Z_2 with increasing ε. One can see that only relatively large values of ε can destabilize the system. However, in the case of slow migration of predators the regulation in the system will take place via a different scenario since (i) the distribution of predator densities no longer follow the distribution of food closely and (ii) the oscillations (damped or sustained) are no longer synchronized in space (we do not show this result for the sake of brevity). In particular, large deviations from (9) are observed for the oscillatory dynamics; however, trajectories of the system are still bounded. This scenario of regulation of an otherwise unbounded system with slow moving of predators should be considered elsewhere.

We also saw that top-down control remains efficient in the case where the prey is allowed to migrate as well, provided the rate of migration is small. Intensive migration of prey, however, will lead to destabilization of the system, a fact which can be understood

intuitively, since prey migration has a tendency to make the system more homogeneous. In particular, it causes the distribution of prey and the resultant distribution of predators to become more even among the sites, thus making the trophic pressure of predators more site-independent, which prevents accumulation of on the sites with maximal food abundance to efficiently suppress prey outbreaks. On the other hand, in the case where migration of the prey is faster than that of the predators this can have a stabilizing effect (e.g. Murdoch et al. (1992)), but the stabilization of the system in this case is due to asynchrony of species oscillations in the sites (Ives, 1992; Murdoch et al., 1992). Overall, a comprehensive comparison of the stabilization/destabilization of metapopulation predator–prey models within a wide range of ratios between the migration rates of prey and predator would be an interesting topic for future research.

5.2. Taking into account more complex distributions of predators

So far we have considered that the instantaneous distribution of predators follows the relative proportion of the amount of food in the sites (see (9)). In real ecosystems, however, this simple relation can be violated, for example, by interference among predators or parasitoids in sites containing large amounts of prey or hosts (Hassell and May, 1973; Sutherland, 1983; Latto and Hassell, 1988). This situation requires the implementation of more complicated models, but some preliminary conclusions on the influence of predator interference on the ecosystem's stability can be made using a fairly simple parameterization (Murdoch et al., 1992):

$$\tilde{Z}_i = \frac{P_i^\mu}{\sum_i P_i^\mu} Z, \quad \mu > 0, \tag{18}$$

where the parameter $\mu > 0$ describes for the strength of the interference.

Our analysis of the system with $\tilde{Z}_i$ given by (18) shows that increasing the interference (decreasing the value of μ) of predators starting from $\mu = 1$ has a destabilizing effect. We found that the size of the domain of stabilization in the parametric space shrinks as μ decreases. On the contrary, an increase in μ ($\mu > 1$) initially results in an enhancement of stability for intermediate values of μ, although a further increase of μ leads to shrinking of the size of the stability domain. A similar response of the stability properties to an increase of μ was previously found in a predator–prey system with slow migration of predators (Murdoch et al., 1992). The authors of the cited paper interpret μ as a degree of predator aggregation, and relate the decrease in stability to a more pronounced synchronization of local oscillations on the sites, but in our case this explanation does not seem to work since the local oscillations of prey density are synchronous.

We can explain the observed destabilization for a low degree of interference (high degree of aggregation) by noting that for large μ the system becomes more homogeneous due to the interplay between the predation and the growth rate. To better illustrate our idea, let us consider a two-site system. Suppose we have pronounced heterogeneity in prey distribution, i.e., that P_2/P_1 largely deviates from 1, then this would signify that for large μ the predation in the site with smaller density will be close to zero, i.e., the predation in this site will be 'switched off'. This can be directly seen from the expression for predation

$$f(P_i)\frac{P_i^\mu}{P_1^\mu + P_2^\mu} Z \approx f(P_i)\left(\frac{P_i}{P_j}\right)^\mu Z \ll 1 \quad \text{for } P_j/P_i > 1. \tag{19}$$

In this case, the prey species in the site with smaller density will show an exponential growth until the densities in both sites are close to each other $P_2/P_1 \approx 1$, and as a result, the oscillations of species densities will become synchronized and, more importantly the species densities will be close to each others. In this case, the resultant system will be a simple predator–prey model for the total amounts of prey and predator $P = P_1 + P_2 \approx 2P_2 \approx 2P_1$ and Z with predator functional response $f(P)$ of Holling type II ($\beta > 0$) and it is well known that such a system is globally unstable. Thus, the main factor resulting in system destabilization, for large μ is spatial homogenization and not synchronization.

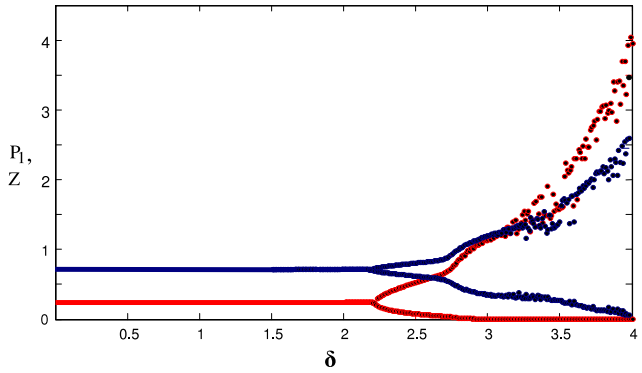

Fig. 5. Influence of a delay in the distribution predators (9) across the sites on the stability of model (10)–(11), $n = 2$. The time lag δ between the distribution of predators and the actual food density is described by (20). The diagram shows stationary biomasses of the stable stationary state and the maximal/minimal species biomasses along the limit cycle for P_1 (in red) and Z (in blue). The model parameters are $\alpha = 2$, $k = 0.25$, $\beta = 0.1$; $m = 0.1$, $r_1 = 1$; $r_2 = 0.3$. (For interpretation of the references to colour in this figure legend, the reader is referred to the web version of this article.)

Apart from interference among the predators, a deviation from the predator distribution term (9) can be caused by other factors, such as a time lag between changes in the distribution of food and that of predators. For instance, this can happen when one models interactions in planktonic ecosystems in the water column. It is well known that the grazers in such systems need time to adjust their distribution to variation in the profile of chlorophyll (Bollens and Frost, 1989; Ohman, 1990). This scenario can be modeled by the following function with a delay

$$\tilde{Z}_i(\tau) = \frac{P_i(\tau - \delta)}{\sum_i P_i(\tau - \delta)} Z(\tau), \tag{20}$$

where δ is the delay parameter.

This case is similar to (9), but with distribution based on the information on the food densities in sites in the past can. We investigated how such a delay can alter the stability properties and found that small values of δ do not change the stability; however, a supercritical time lag can result in system destabilization – a rather typical behavior for systems with delay (cf. Arditi et al., 1977; Hastings, 1984). We illustrate the influence of the delay in Fig. 5, which is constructed for a two-site system (10)–(11) for $r_1 = 1$; $r_2 = 0.3$; $\beta = 0.1$. After the loss of stability at $\delta \approx 2.2$, a further increase in the delay results in a cascade of the period-doubling bifurcation, and finally can lead to chaotic oscillations. Despite this loss of stability, the system is still regulated in the sense that the oscillations are bounded. However, the persistence of the species becomes humped with an increase of δ because the prey biomass is extremely low at the minima of the population cycles. In Appendix E, we estimate analytically the critical threshold of destabilizing delay δ in the model (10)–(11) for linear functional response $\beta = 0$, which can guarantee system stabilization.

5.3. Ecological applications

The obtained theoretical results can shed some light on explaining the phenomenon which is known as 'the paradox of

enrichment' (Rosenzweig, 1971; Gilpin, 1972; Scheffer and De Boer, 1995; McCauley et al., 1999; Roy and Chattopadhyay, 2007). This paradox arises when an increase in the carrying capacity of the ecosystem results in large-amplitude oscillations of the predator–prey interactions, thus in ecosystems with a high degree of eutrophication top-down control becomes inefficient. A large number of field data contradict these predictions, suggesting some as-yet unknown robust mechanisms of top-down control (Abrams and Walters, 1996; McCauley et al., 1999; Genkai-Kato and Yamamura, 2000). An important example of the paradox of enrichment concerns regulations of the nutrient-rich low chlorophyll open ocean regions (Chavez et al., 1990; Armstrong, 1994), where a low density of phytoplankton is observed throughout the year despite a very high concentration of limiting nutrients. This paradoxical behavior is still a matter of intensive discussions (Lancelot et al., 2000; Boyd, 2002) and different mechanisms of regulation have been suggested. The dynamics of the nutrient-rich high chlorophyll ecosystems provides us with an important case study for applications of the theoretical results obtained in this paper.

Planktonic communities are highly heterogeneous in space; this especially concerns the distribution of species in the water column: due to the attenuation of light with depth there is a pronounced gradient in the algal growth rate. On the other hand, herbivorous zooplankton is capable of rapid vertical migration and may adjust its vertical location according to the food availability and other factors (Boyd et al., 1980; Dagg et al., 1997; Morozov et al., 2007). The vertical zooplankton distribution in the water column can be approximately described by distribution (9) (Leising and Franks, 2000; Lampert, 2005; Morozov, 2010). Interestingly, in a large number of eutrophic marine ecosystems, regulation of algal growth takes place by an intermediate predator, the microzooplankton (Calbet and Landry, 2004; Irigoien et al., 2005) – in other words, phytoplankton is mostly being grazed by microzooplankton with the growth rate occurring on the same time scale as that of algae (the characteristic time scale is of several hours). Microzooplankton are, in turn, consumed by mesozooplankton (copepods) which have a slow growth rate (the characteristic scale varies from one month to one year). Rather than the limited movement capability of most of phytoplankton and microzooplankton species, mesozooplankters usually show fast vertical displacement within the entire water column (Dagg et al., 1997).

For the above reasons, interactions of phytoplankton and micro- and meso-zooplankton in nutrient-rich waters can be described by model (15)–(16), where only the top predator is allowed to migrate. The required model parameters can be estimated from the literature (Edwards and Brindley, 1999; Leising et al., 2003; Saiz and Calbet, 2007). For the sake of simplicity, we consider species interactions in the water column with the depth of the euphotic zone 100 m. We divide the euphotic zone into 2 layers ('sites'), and we consider that the phytoplankton growth rates are $r_1 = 1$ 1/d and $r_2 = 0.3$ 1/d in the surface layer and the deep layer, respectively (cf. Morozov and Arashkevich, 2008). The zooplankton grazing parameters can be estimated as $a_N = 2$ 1/(d μg C l^{-1}); 0.01 1/(μg C l^{-1}) $< b_N, \beta <$ 0.2 1/(μg C l^{-1}); 0.01 1/(d μg C l^{-1}) $< \alpha <$ 0.3 1/(d μg C l^{-1}) (the unit of plankton density is chosen as μg C l^{-1}) and the density of mesozooplankton Z is a free parameter, we consider it to vary in the following range 1 μg C $l^{-1} < Z <$ 20 μg C l^{-1} which gives $0.01 < M < 6$ 1/d. By substituting the above estimates into (15)–(16) we find that the system is stable within a large range of realistic parameters. Thus, regulation of tri-trophic phytoplankton–microzooplankton–mesozooplankton food webs in the eutrophic waters can be potentially explained based on the reported mechanism of top-down control. Furthermore, including realistic vertical diffusion of phytoplankton into the model (i.e., allowing the phytoplankton to move in space) does not influence the above results on stabilization. In particular, the P–Z interactions in the column with distribution of zooplankton given by (9) were modeled numerically via a continuous PDEs framework (Morozov et al., 2011) with the vertical diffusion coefficient for phytoplankton given by $D = 1$ m^2/d, and stabilization of this system with an unlimited nutrient stock was found within a large range of realistic parameters.

We should emphasize that the ecological applications of our results are not limited to interaction in planktonic communities in the water column – other species show fast migration resulting in a distribution which is close to (9) (Milinski, 1979; Godin and Keenleyside, 1984; Bernstein et al., 1988; Kacelnik et al., 1992; Milinski, 1994; Bernstein et al., 1999; Nachman, 2006). In the cited works, the predator–prey pairs are algae/zooplankton–fish, insects–birds, aphids–aphids predators/parasitoids, acarine predator–prey systems. We should emphasize that the reported mechanism of stabilization does not require the prey population to be sessile or almost sessile, provided that the ratio between the mobility of predators and that of preys is sufficiently large. In particular, model (15)–(16) can be applied to investigate the stabilizing effects of predation by fish (fast moving top predator) in coastal aquatic ecosystems. In this case, the population dynamics of coastal and pelagic zones become coupled by a rapid food-mediated migration of fish which can assure extra stability in those systems (Lodge et al., 1988). The same holds true for modeling interactions between pelagic and benthic communities, where fast moving top predators can potentially play a role in stabilizing the community dynamics (Boero et al., 1996).

Acknowledgments

We highly appreciate the editor of the journal, Peter Chesson, for providing valuable comments and suggestions which helped us to improve the manuscript. M. Sen is thankful to CSIR, India for providing a senior research fellowship.

Appendix A

Here we show that system (10)–(11) has a unique interior stationary state. The stationary biomasses are determined from

$$0 = r_i - f\left(P_i^*\right)\frac{1}{\sum_i P_i^*}Z^*, \quad i = 1, n \tag{A.1}$$

$$0 = k\sum_i f\left(P_i^*\right)\frac{P_i^*}{\sum_i P_i^*} - m, \tag{A.2}$$

where $f(P)$ is given by (3). We multiply each equation in (A.1) by P_i^* and sum up the obtained equations. By combining the resultant sum with (A.2), we can easily compute the stationary total biomass of predator

$$Z^* = \frac{k\sum_i r_i}{k\alpha - m\beta}. \tag{A.3}$$

The stationary biomasses P_i^* of prey cannot be obtained explicitly. It is easy to prove that all are laying in the following hyperplane

$$Z^*\frac{m}{k} = r_1P_1^* + r_2P_2^* + \cdots + r_nP_n^*. \tag{A.4}$$

From (A.1), it can be easily derived that

$$r_i\left(1 + \beta P_i^*\right)\left(\sum_i P_i^*\right) = \alpha\, Z^*P_i^* \quad i = 1, n. \tag{A.5}$$

Thus, P_i^* can be expressed as a function of P_1^*

$$P_i^* = r_i \frac{P_1^*}{r_1 + \beta (r_1 - r_i) P_1^*} \quad i = 2, n. \tag{A.6}$$

For the sake of simplicity we assume that the patch 1 is characterized by the maximal growth rate of prey, i.e., $r_1 > r_i, i > 1$. We plug (A.6) into (A.4) and obtain the algebraic equation for P_1^* which is given by

$$\omega_0 \left(P_1^*\right)^n + \omega_1 \left(P_1^*\right)^{n-1} + \cdots + \omega_n = 0, \tag{A.7}$$

where the coefficients ω_0, ω_n are determined by

$$\begin{aligned} \omega_0 &= \beta \left(r_1 \sum_{i \neq 1} (r_1 - r_i) + r_2 \sum_{i \neq 2} (r_1 - r_i) + \cdots \right. \\ &\quad \left. + \; r_n \sum_{i \neq n} (r_1 - r_i) \right) > 0, \\ \omega_n &= -Z^* \frac{m}{k} (r_1)^{n-1} < 0. \end{aligned} \tag{A.8}$$

From (A.8) it can be easily seen that Eq. (A.7) has, at least, one positive root, this proves the existence of an interior stationary state $(P_1^*, P_2^*, \ldots, P_n^*, Z^*)$. This positive solution is unique. Indeed, suppose that there exists another stationary state $(\tilde{P}_1^*, \tilde{P}_2^*, \ldots, \tilde{P}_n^*, Z^*)$ with $\tilde{P}_1^* > P_1^*$. From (A.6) it follows that $\tilde{P}_i^* > P_i^*$, $i > 2$. It contradicts, however, condition (A.4) which states that all stationary values of prey biomass should be located on the mentioned hyperplane.

One can obtain the explicit expression for the interior stationary state in the particular case, when the functional response is linear ($\beta = 0$):

$$P_i^* = \frac{d r_i \sum\limits_i r_i}{k\alpha \sum\limits_i r_i^2}, \qquad Z^* = \frac{\sum\limits_i r_i}{\alpha}, \quad i = 1, n. \tag{A.9}$$

In the case, where growth rates on all sites are the same ($r_1 = r_2 = r$), we have

$$P_i^* = \frac{d}{k\alpha - m\beta}, \qquad Z^* = \frac{k n r}{k\alpha - m\beta} \quad i = 1, n. \tag{A.10}$$

Appendix B

Here we consider the particular case of model (10)–(11), $n = 2$ in the case where the functional response is linear: $\beta = 0$. The model equations become

$$\frac{dP_i}{dt} = r_i P_i - \alpha \frac{P_i^2}{\sum\limits_i P_i} Z, \tag{B.1}$$

$$\frac{dZ}{dt} = \left(k \sum_{i=1}^{2} \alpha \frac{P_i^2}{\sum\limits_i P_i} - m \right) Z, \quad n = 2. \tag{B.2}$$

We are interested in the stability properties of the interior stationary state. The coordinates of the stationary state are given by (A.9). The Jacobian matrix computed at this stationary state is determined by

$$J_2 = \begin{pmatrix} -\frac{r_1 r_2}{r_1 + r_2} & \frac{r_1^2}{r_1 + r_2} & -\frac{d r_1^2}{k\left(r_1^2 + r_2^2\right)} \\ \frac{r_2^2}{r_1 + r_2} & -\frac{r_1 r_2}{r_1 + r_2} & -\frac{d r_2^2}{k\left(r_1^2 + r_2^2\right)} \\ k\left(r_1 + r_2 - \frac{2 r_2^2}{k(r_1 + r_2)}\right) & k\left(r_1 + r_2 - \frac{2 r_1^2}{k(r_1 + r_2)}\right) & 0 \end{pmatrix}. \tag{B.3}$$

The characteristic equation for the eigen values of (B.3) is the following

$$\lambda^3 + A_1 \lambda^2 + A_2 \lambda + A_3 = 0, \tag{B.4}$$

where the polynomial coefficients A_i are given by

$$\begin{aligned} A_1 &= \frac{2 r_1 r_2}{r_1 + r_2}; \\ A_2 &= d \left(r_1 + r_2 - \frac{4 r_1^2 r_2^2}{(r_1 + r_2)\left(r_1^2 + r_2^2\right)} \right); \\ A_3 &= d r_1 r_2. \end{aligned} \tag{B.5}$$

It is easy to verify that $A_i > 0, i = 1, 3$. Computation of $A_1 A_2 - A_3$ gives

$$\begin{aligned} &A_1 A_2 - A_3 \\ &\quad = \frac{d r_1 r_2}{(r_1 + r_2)\left(r_1^2 + r_2^2\right)} \left((r_1 + r_2)^2 \left(r_1^2 + r_2^2\right) - 8 r_1^2 r_2^2 \right) > 0. \end{aligned} \tag{B.6}$$

Thus, according to the Routh–Hurwitz stability criterion the nontrivial stationary state of the model is always stable (at least, locally) in case of the linear functional response. Note that in the case $r_1 = r_2$ the equilibrium becomes neutrally stable since $A_1 A_2 - A_3 = 0$.

Appendix C

Here we consider a special form of model system (10)–(11) for a two-site system with the assumption that $r_1 = r_2$ (i.e., the habitat is homogeneous). Under this assumption, the model becomes

$$\frac{dP_i}{dt} = r P_i - \frac{1}{1 + \beta P_i} \frac{P_i^2}{\sum\limits_i P_i} Z, \tag{C.1}$$

$$\frac{dZ}{dt} = \left(k \sum_{i=1}^{2} \frac{1}{1 + \beta P_i} \frac{P_i^2}{\sum\limits_i P_i} - m \right) Z. \tag{C.2}$$

The coordinates of the interior stationary state are given by (A.10). The Jacobian matrix computed at this stationary state is given by

$$J_1 = \begin{pmatrix} -\frac{r(k\alpha - 2\beta m)}{2k\alpha} & \frac{r}{2} & -\frac{d}{2k} \\ \frac{r}{2} & -\frac{r(k\alpha - 2\beta m)}{2k\alpha} & -\frac{d}{2k} \\ \frac{r(k\alpha - 2\beta m)}{\alpha} & \frac{r(k\alpha - 2\beta m)}{\alpha} & 0 \end{pmatrix}. \tag{C.3}$$

The characteristic equation for the eigen values of (C.3) is the following

$$\lambda^3 + B_1 \lambda^2 + B_2 \lambda + B_3 = 0, \tag{C.4}$$

where the polynomial coefficients B_i are described by

$$\begin{aligned} B_1 &= \frac{r(k\alpha - 2m\beta)}{k\alpha}; \\ B_2 &= -\frac{m r (k\alpha - m\beta)(r\beta - k\alpha)}{k^2 \alpha^2}; \\ B_3 &= \frac{(k\alpha - m\beta)^2 m r^2}{k^2 \alpha^2}. \end{aligned} \tag{C.5}$$

The Routh–Hurwitz criterion of stability implies $B_i > 0, B_1 B_2 - B_3 > 0$. It is easy to verify that $B2 > 0$; $B3 > 0$. The condition $B1 > 0$ requires that $k\alpha > 2m\beta$. Computation of $B_1 B_2 - B_3$ gives

$$\begin{aligned} &B_1 B_2 - B_3 \\ &\quad = -\frac{r^2 m \beta}{k^3 \alpha^3} (r(k\alpha - 2m\beta) + mk\alpha)(k\alpha - m\beta) < 0 \end{aligned} \tag{C.6}$$

wherever $B1 > 0$. Thus, the interior stationary state of the model is always unstable for $r_1 = r_2$.

Appendix D

Here we analyze the stability of the interior stationary state of model (16)–(17), $n = 2$ and the linear functional responses of intermediate predator and top predator. The stationary biomasses of species are determined by

$$N_i^* = \frac{r_i}{k\alpha \sum\limits_i r_i} M\gamma; \qquad P_i^* = r_i/\alpha, \quad i = 1, 2. \tag{D.1}$$

The Jacobian matrix computed at this stationary state is given by

$$J_3 = \begin{pmatrix} 0 & 0 & -\dfrac{r_1}{k\,(r_1+r_2)} M\gamma & 0 \\ 0 & 0 & 0 & -\dfrac{r_2}{k\,(r_1+r_2)} M\gamma \\ r_1 k & 0 & -\dfrac{r_1 r_2}{(r_1+r_2)^2} M\gamma & \dfrac{r_1^2}{(r_1+r_2)^2} M\gamma \\ 0 & r_2 k & \dfrac{r_1^2}{(r_1+r_2)^2} M\gamma & -\dfrac{r_1 r_2}{(r_1+r_2)^2} M\gamma \end{pmatrix}. \tag{D.2}$$

The characteristic equation for the eigen values of (D.2) is the following

$$\lambda^4 + C_1\lambda^3 + C_2\lambda^2 + A_3\lambda + A_4 = 0, \tag{D.3}$$

where the polynomial coefficients C_i are given by

$$\begin{aligned} C_1 &= \frac{2r_1r_2}{(r_1+r_2)^2} M\gamma, \qquad C_2 = \frac{r_1^2+r_2^2}{(r_1+r_2)} M\gamma, \\ C_3 &= r_1r_2 \frac{r_1^2+r_2^2}{(r_1+r_2)^3} (M\gamma)^2, \qquad C_4 = \frac{r_1^2 r_2^2}{(r_1+r_2)^2} (M\gamma)^2. \end{aligned} \tag{D.4}$$

It is easy to see that $C_i > 0, i = 1, 4$. The Routh–Hurwitz stability criterion requires that $C_1C_2C_3 - C_3^2 - C_1^2C_4 > 0$. After some simplification we derive

$$C_1C_2C_3 - C_3^2 - C_1^2C_4 = \frac{(M\gamma)^2}{(r_1+r_2)^2} r_1^2 r_2^2 > 0. \tag{D.5}$$

Thus, the interior stationary state is always stable.

Appendix E

Here we consider the influence of a delay in the ideal free distribution of predator (described by (20)) on the stability of the interior stationary state of model (10)–(11). The coordinates of the stationary state are the same as in the system without delay and are given by (A.10). We use a standard approach of stability analysis of ODEs with delay (Dieudonne, 1960; Bairagi et al., 2008). The characteristic equation of the linearized system in the vicinity of the stationary state is given by

$$\lambda^3 + F_1\lambda^2 e^{-\lambda\delta} + \lambda\left(F_2 + F_3 e^{-\lambda\delta}\right) + F_4 e^{-\lambda\delta} = 0, \tag{E.1}$$

where $F_1 = \frac{2r_1r_2}{r_1+r_2}$, $F_2 = \frac{d\left(r_1^3+r_2^3\right)}{r_1^2+r_2^2}$, $F_3 = \frac{d\,r_1r_2(r_1-r_2)^2}{\left(r_1^2+r_2^2\right)(r_1+r_2)}$, $F_4 = dr_1r_2$. It is easy to see that $F_i > 0$. The local stability of the stationary state is determined by the sign of the characteristic root of Eq. (E.1). However, Eq. (E.1) is a transcendental equation and the Routh–Hurwitz stability criterion cannot be applied directly. By substituting $\lambda = \mu + i\sigma$ and separating the real and the imaginary parts, we obtain

$$\begin{aligned} &\mu^3 - 3\mu\sigma^2 + F_2\mu + e^{-\mu\delta}\left[\left\{F_1\left(\mu^2-\sigma^2\right) + F_3\mu + F_4\right\}\right. \\ &\quad \left. \times \cos\sigma\delta + \left\{2F_1\mu\sigma + F_3\sigma\right\}\sin\sigma\delta\right] = 0, \end{aligned} \tag{E.2}$$

$$\begin{aligned} &3\mu^2 - \sigma^3 + F_2\sigma + e^{-\mu\delta}\left[\left\{2F_1\mu\sigma + F_3\sigma\right\}\cos\sigma\delta\right. \\ &\quad \left. - \left\{F_1\left(\mu^2-\sigma^2\right) + F_3\mu + F_4\right\}\sin\sigma\delta\right] = 0. \end{aligned} \tag{E.3}$$

The existence of a pair of purely imaginary roots $\lambda = \pm i\sigma$ of the characteristic Eq. (E.1) would imply the change of stability of the stationary state. We consider δ as a bifurcation parameter (note that for $\delta = 0$ the system is table and $\mu < 0$, see Appendix B). The stability change at $\delta = \delta_0$ will signify that $\mu(\delta_0) = 0$ and $\sigma(\delta_0) = \sigma_0$. Thus, at $\delta = \delta_0$ we have

$$\left(F_1\sigma_0^2 - F_4\right)\sin\sigma_0\delta_0 + F_3\sigma_0\cos\sigma_0\delta_0 = \sigma_0^3 - F_2\sigma_0, \tag{E.4}$$

$$\left(F_1\sigma_0^2 - F_4\right)\cos\sigma_0\delta_0 - F_3\sigma_0\sin\sigma_0\delta_0 = 0. \tag{E.5}$$

We eliminate the trigonometric terms in (E.4)–(E.5) and obtain

$$\begin{aligned} \Phi\left(\sigma_0^2\right) \equiv\ &\sigma_0^6 - \left(2F_2 + F_1^2\right)\sigma_0^4 \\ &+ \left(F_2^2 + 2F_1F_1 - F_3^2\right)\sigma_0^4 - F_4^2 = 0. \end{aligned} \tag{E.6}$$

It easy to see that the cubic equation (E.6) has at least one positive real root. Let us denote the smallest positive root of this equation by $\delta = \delta_0$, the corresponding pair of imaginary roots $\lambda = \pm i\sigma_0$. Thus, the critical magnitude of the delay parameter is

$$\delta_0(n) = \frac{1}{\sigma_0}\tan^{-1}\left(\frac{F_1\sigma_0^2 - F_4}{F_3} + \frac{n\pi}{\sigma_0}\right), \quad n = 0, 1, 2\ldots. \tag{E.7}$$

Thus, the initially stable stationary state ($\delta = 0$) system becomes unstable when δ is being increased and passes through $\delta_0(n)$. We also found that the system undergoes a Hopf bifurcation at $\delta = \delta_0(n)$ by checking the transversality conditions (Kuznetsov, 1995). We do not show this result for the sake of brevity.

References

El Abdllaoui, A., Auger, P., Kooi, B.W., Bravo de la Parra, R., Mchich, R., 2007. Effects of density-dependent migrations on stability of a two-patch predator–prey model. Math. Biosci. 10, 335–354.

Abrams, P.A., 1990. The effects of adaptive behavior on the type-2 functional response. Ecology 71, 877–885.

Abrams, P.A., Walters, C.J., 1996. Invulnerable prey and the paradox of enrichment. Ecology 77, 1125–1133.

Abta, R., Shnerb, N.M., 2007. Angular velocity variations and stability of spatially explicit prey–predator systems. Phys. Rev. E. 75, 051914.

Armstrong, R.A., 1994. Grazing limitation and nutrient limitation in marine ecosystems: steady state solutions of an ecosystem model with multiple food chains. Limnol. Oceanogr. 39, 597–608.

Arditi, R., Abbilon, J.-M., Viviera da Silva, J., 1977. The effect of a time-delay in a predator–prey model. Math. Biosci. 33, 107–120.

Auger, P., Charles, S., Viala, M., Poggiale, J.C., 2000. Aggregation and emergence in ecological modelling: integration of ecological levels. Ecol. Mod. 127, 11–20.

Bairagi, N., Sarkar, R.R., Chattopadhyay, J., 2008. Impacts of incubation delay on the dynamics of an eco-epidemiological system-a theoretical study. Bull. Math. Biol. 70, 2017–2038.

Beddington, J.R., Free, C.A., Lawton, J.H., 1978. Modelling biological control: on the characteristics of successful natural enemies. Nature 273, 513–519.

Bernstein, C., Kacelnik, A., Krebs, J., 1988. Individual decisions and the distribution of predators in a patchy environment. J. Animal Ecol. 57, 1007–1026.

Bernstein, C., Auger, P., Poggiale, J.C., 1999. Predator migration decisions, the ideal free distribution and predator–prey dynamics. Am. Nat. 153, 267–281.

Boero, E., Belmonte, G., Fanelli, G., Piraino, S., Rubino, F., 1996. The continuity of living matter and the discontinu-ities of its constituents: do plankton and benthos really exist? Trends Ecol. Evol. 11, 177–180.

Bollens, S.M., Frost, B.W., 1989. Predator induced diel vertical migration in a marine planktonic copepod. J. Plankton Res. 11, 1047–1065.

Boyd, C.M., Smith, S.M., Cowles, T., 1980. Grazing patterns of copepods in the upwelling system off Peru. Limnol. Oceanogr. 25, 583–596.

Boyd, P.W., 2002. Environmental factors controlling phytoplankton processes in the Southern Ocean. J. Phycol. 38, 844–861.

Briggs, C.J., Hoopes, M.F., 2004. Stabilizing effects in spatial parasitoid–host and predator–prey models: a review. Theor. Popul. Biol. 65, 299.

Calbet, A., Landry, M., 2004. Phytoplankton growth, microzooplankton grazing, and carbon cycling in marine systems. Limnol. Oceanogr. 49, 51–57.
Chavez, F.P., Buck, K.R., Barber, R.T., 1990. Phytoplankton taxa in relation to primary production in the equatorial Pacific. Deep Sea Res. 37, 1733–1752.
Chesson, P.L., Murdoch, W.W., 1986. Aggregation of risk: relationships among host–parasitoid models. Am. Nat. 127, 696–715.
Cuddington, K.M., McCauley, E., 1994. Food-dependant aggregation and mobility of water fleas Ceriodaphnia and Daphia pullex. Can. J. Zool. 72, 1217–1226.
Dagg, M.J., Frost, B.W., Newton, J.A., 1997. Vertical migration and feeding behavior of Calanus pacificus females during a phytoplankton bloom in Dabob Bay, US. Limnol. Oceanogr. 42, 974–980.
Dhooge, A., Govaerts, W., Kuznetsov, Y., 2003. Matcont: a matlab package for numerical bifurcation analysis of odes. ACM Toms 29, 141–164. URL:http://sourceforge.net/projects/matcont/.
Dieudonne, J., 1960. Foundations of Modern Analysis. Academic, New York.
Edwards, A.M., Brindley, J., 1999. Zooplankton mortality and the dynamical behavior of plankton population models. Bull. Math. Biol. 61, 202–339.
Genkai-Kato, M., Yamamura, N., 2000. Profitability of prey determines the response of population abundances to enrichment. Proc. R Soc. Lond. B 267, 2397–2401.
Gilpin, M.E., 1972. Enriched predator–prey systems: theoretical stability. Science 177, 902–904.
Godfray, H.C.J., Pacala, S.W., 1992. Aggregation and the population dynamics of parasitoids and predators. Am. Nat. 140, 30–40.
Godin, J.G.J., Keenleyside, M.H.A., 1984. Foraging on patchy distributed prey by a cichlid fish, Teleostei, Cichlidae: a test of the ideal free distribution theory. Animal Behavior 32, 120–131.
Hastings, A., 1984. Delays in recruitment at different trophic levels effects on stability. J. Math. Biol. 21, 35–44.
Hassell, M.P., 1978. The Dynamics of Arthropod Predator–Prey systems. Princeton University Press, Princeton, NJ.
Hassell, M.P., May, R.M., 1973. Stability in insect host–parasite models. J. Anim. Ecol. 42, 693–736.
Hassell, M.P., May, R.M., 1974. Aggregation in predators and insect parasites and its effect on stability. J. Anim. Ecol. 43, 567–594.
Hassell, M.P., May, R.M., Pacala, S.W., Chesson, P.L., 1991. The persistence of host–parasitoid associations in patchy environments: I, a general criterion. Am. Nat. 138, 568–583.
Hassell, M.P., 2000. Host–parasitoid population dynamics, 2000. J. Anim. Ecol. 69, 543–566.
Hogarth, W.L., Diamond, P., 1984. Interspecific competition in larvae between entamophagous parasitoids. Am. Nat. 124, 552–560.
Holling, C.S., 1959. The components of predation as revealed by a study of small-mammal predation of the European pine sawfly. Canad. Entomologist 91, 293–320.
Irigoien, X., Flynn, K.J., Harris, R.P., 2005. Phytoplankton blooms: a loophole in microzooplankton grazing impact? J. Plankton Res. 27, 313–321.
Ives, A.R., 1992. Continuous-time models of host-parasitoid interactions. Am. Nat. 140, 1–29.
Jakobsen, P.J., Johnsen, G.H., 1987. Behavioral response of the waterflea Daphia pulex to a gradient in food concentration. Animal Behavior 35, 48–52.
Jeschke, J.M., Kopp, M., Tollrian, R., 2002. Predator functional responses: discriminating between handling and digesting prey. Ecol. Monogr. 72, 95–112.
Kacelnik, A., Krebs, J.R., Bernstein, C., 1992. The ideal free distribution and predator–prey populations. Trends Ecol. Evol. 7, 50–55.
Kuznetsov, Y.A., 1995. Elements of Applied Bifurcation Theory. Springer, Berlin, Heidelberg, New York.
Lampert, W., 2005. Vertical distribution of zooplankton: density dependence and evidence for an ideal free distribution with costs. BMC Biology 3 10, (electronic).
Lancelot, C., Hannon, E., Bequevort, S., Veth, C., De Baar, H.J.W., 2000. Modeling phytoplankton blooms and carbon export production in the Southern Ocean: dominant controls by light and iron in the Atlantic sector in Austral spring 1992. Deep Sea Res. I 47, 1621–1662.
Larsson, P., 1997. Ideal free distribution in Daphnia? are daphnids able to consider both patch quality and the position of competitors? Hydrobiologia 360, 143–152.
Latto, J., Hassell, M.P., 1988. Generalist predators and the importance of spatial density dependence. Oecologia 77, 375–377.
Leising, A.W., Franks, P.J.S., 2000. Copepod vertical distribution within a spatially variable food source: a foraging strategy model. J. Plankton Res. 22, 999–1024.
Leising, A.W., Gentleman, W.C., Frost, B.W., 2003. The threshold feeding response of microzooplankton within Pacific high nitrate low-chlorophyll ecosystem models under steady and variable iron input. Deep-Sea Res. II 50, 2877–2894.
Lodge, D.M., Barko, J.W., Strayer, D., Melack, J.M., Mittelbach, G.G., Howarth, R.W., Menge, B., Titus, J.E., 1988. Spatial heterogeneity and habitat interactions in lake communities. In: Carpenter, S.R. (Ed.), Complex Interactions in Lake Communities. Springer-Verlag, New York, New York, USA, pp. 181–227.
May, R.M., Hassell, M.P., 1981. The dynamics of multiparasitoid–host interactions. Am. Nat. 117, 308–315.
McCauley, E., Nisbet, R.M., Murdoch, W.W., De Roos, A.M., Gurney, W.S.C., 1999. Large amplitude cycles of daphnia and its algal prey in enriched environments. Nature 402, 653–656.
Milinski, M., 1979. An evolutionarily stable feeding strategy in sticklebacks. Z. Tierpsychol. 51, 36–40.
Milinski, M., 1994. Long-term memory for food patches and implications for ideal free distributions in sticklebacks. Ecology 75, 1150–1156.
Morozov, A.Y., Petrovskii, S.V., Nezlin, N.P., 2007. Towards resolving the paradox of enrichment in plankton community: role of zooplankton vertical migration. J. Theor. Biol. 248, 501–511.
Morozov, A.Y., Arashkevich, A.G., 2008. Patterns of zooplankton functional response in communities with vertical heterogeneity: a model study. Math. Model. Nat. Phenom. 3, 131–148.
Morozov, A.Yu., 2010. Emergence of Holling type III zooplankton functional response: bringing together field evidence and mathematical modelling. J. Theor. Biol. 265, 45–54.
Morozov, A.Yu., Arashkevich, E.G., Nikishina, A., Solovyev, K., 2011. Nutrient-rich plankton communities stabilized via predator–prey interactions: revisiting the role of vertical heterogeneity. Math. Med. Biol. 28, 185–215.
Murdoch, W.W., Oaten, A., 1975. Predation and population stability. Adv. Ecol. Res. 9, 1–131.
Murdoch, W.W., Briggs, C.J., Nisbet, R.M., Gurney, W.S.C., Stewart-Oaten, A., 1992. Aggregation and stability in metapopulation models. Am. Nat. 140, 41–58.
Murdoch, W.W., Stewart-Oaten, A., 1989. Aggregation by parasitoids and predators: effects on equilibrium and stability. Am. Nat. 134, 228–310.
Nachman, G., 2006. A functional response model of a predator population foraging in a patchy habitat. J. Anim. Ecol. 75, 948–958.
Oaten, A., Murdoch, W.W., 1975. Functional response and stability in predator–prey systems. Am. Nat. 109, 289–298.
Ohman, M.D., 1990. The demographic benefits of diel vertical migration by zooplankton. Ecol. Monogr. 60, 257–281.
Pulido, F., Díaz, M., 1997. Linking individual foraging behavior and population spatial distribution in patchy environments: a field example with Mediterranean blue tits. Oecologia 111, 434–442.
Rohani, P., Godfray, H.C.J., Hassell, M.P., 1994. Aggregation and the dynamics of host–parasitoid systems: a discrete generation model with within-generation redistribution. Am. Nat. 144, 491–509.
Rosenzweig, M.L., 1971. Paradox of enrichment: destabilization of exploitation ecosystems in ecological time. Science 171, 385–387.
Roy, S., Chattopadhyay, J., 2007. The stability of ecosystems: a brief overview of the paradox of enrichment. J. Biosci. 32, 421–428.
Saiz, E., Calbet, A., 2007. Scaling of feeding in marine calanoid copepods. Limnol. Oceanogr. 52, 668–675.
Scheffer, M., De Boer, R.J., 1995. Implications of spatial heterogeneity for the paradox of enrichment. Ecology 76, 2270–2277.
Sutherland, W.J., 1983. Aggregation and the "ideal free" distribution. J. Anim. Ecol. 52, 821–828.
Weisser, W.W., Hassell, M.P., 1996. Animals 'on the move' stabilize host–parasitoid systems. Proc. R Soc. London Ser. B: Biol. 263, 749–754.
Weisser, W.W., Jansen, V.A.A., Hassell, M.P., 1997. The effects of a pool of dispersers on host–parasitoid systems. J. Theor. Biol. 189, 413–425.